Special Issue of the 8th International Advances in Applied Physics and Materials Science Congress (APMAS 2018)

Cavitation Erosion Damage Characteristics of Electroless Nickel Plated Gray Cast Iron

I.C. Park, S.J. Kim*
Mokpo National Maritime University, Division of Marine Engineering, Mokpo, Korea

Cavitation erosion damage behaviors in the coolant of electroless nickel plated diesel engine cylinder liners were investigated. In the case of electroless nickel coating, pitting damage was locally induced by cavitation erosion attacks. The pitting damage was promoted as galvanic corrosion accompanied it. Continued cavitation erosion attacks led to the plastic deformation, fatigue, and failure of electroless nickel coating. Consequently, local pitting damage to electroless nickel coating showed a tendency to progress in the depth direction so that the surface damage depth developed greatly.

DOI: 10.12693/APhysPolA.135.1018
PACS/topics: gray cast iron, electroless nickel plating, cavitation erosion, diesel engine, coolant

1. Introduction

In the case of machinery operated in fluids at high speeds, the fluid pressure is highly likely to drop in areas where the flow velocity is high leading to the formation of cavities so that cavitation damage is highly likely to occur. Fluid pressure locally drops during flows and vapor cavities are formed when the pressure has dropped to below the vapor pressure and disappear when the pressure has risen again. Due to this phenomenon, cavities are formed when vibrations occur on the surfaces of machinery that operate in contact with fluids and cavitation erosion damage is induced in the areas where cavities are formed. A representative case is the cavitation erosion phenomenon of diesel engine cylinder liners surrounded by a coolant [1]. The cavitation erosion phenomenon of cylinder liners is caused by the up-and-down reciprocating motions of the piston in the cylinder liners. At the top dead center (TDC), the drop motion of the piston due to the explosion pressure is transformed into the rotary motion of the crankshaft. As a result, thrust force from the side of the piston becomes to act on the cylinder liners and this is called piston slap. Fast lateral vibrations occur on the cylinder liners due to the repetitive piston slap phenomenon. Consequently, the dynamic pressure of the coolant in contact with cylinder liners rises while the static pressure drops on the contrary. In this case, although the coolant temperature is almost constant, cavitation cavities are formed as the static pressure drops to below the vapor pressure. When the coolant pressure has risen to above the vapor pressure due to continuous changes in the pressure of the cylinder liner coolant, the cavities collapse while generating powerful micro-jets. The repetitive impact pressure of the micro-jets occurred in this case has sufficient kinetic energy to induce material damage of cylinder liners. This phenomenon is called diesel engine cavitation erosion. This cavitation erosion damage eventually becomes to cause penetration damage to cylinder liners and lead the coolant to flow into the inside of the combustion chamber so that the lubricating oil is contaminated resulting in serious damage to the diesel engine. Serious engine damage is frequently caused despite that various surface treatments are applied to prevent cylinder liner cavitation erosion damage. Therefore, understanding surface treated cylinder liners cavitation erosion behavior is very important. This study was intended to understand the cavitation erosion behaviors of electroless nickel (EN) plated cylinder liners in a coolant.

2. Experimental procedure

EN plating was carried out onto GCI which is used for a cylinder liner of the diesel engine. Chemical compositions of gray cast iron are given in Table I. In order to investigate the EN plating properties, specimens (of the size $19.5\times19.5\times5$ mm^3) of gray cast iron were EN plated using the shown parameters in Table II. Ni strike plating was performed to improve the adhesion between the gray cast iron and the EN plating layer. And the heat treatment of the EN plating layer was carried out to alleviate the stress and to improve hardness. For the EN plated specimen, the cavitation-erosion tester with piezoelectric effect was used in engine coolant (Model: TK-6-03-010/2, phosphate type, Sam Yang Chemical Co. Ltd, Korea) environment, and the experiment was conducted by opposite vibration (the so-called 'stationary specimen method') in accordance with the modified ASTM G32 regulations. A 20 kHz rated vibration output was generated through the electronic circuit with 60 Hz, 220 V power, which was supplied to the vibrator. The amplitude was maintained at 50 μm by constant amplitude automatic control. The specimen was fixed in a holder in opposition to the horn of vibrator and a distance of 1 mm was maintained. To minimize the corrosion damage effect of temperature, the coolant temperature was maintained constant at 25 °C during the cavitation-erosion test. Furthermore, for the weight loss analysis, the specimens were

*corresponding author; e-mail: ksj@mmu.ac.kr

cleaned with an ultrasonic cleaner before and after the experiment and dried in a dryer for 24 h at 50 °C. Then their weights were measured and compared. After the cavitation-erosion test, surface damage of the specimens was observed with a scanning electron microscope (SEM) and a 3D microscope. And the micro-Vickers hardness of as-received and EN plated specimens was measured more 10 times and their average values were determined.

TABLE I

Chemical composition of gray cast iron.

Element [wt.%]	C	Si	Mn	P	S
	3.33	1.92	0.76	0.5	0.05
Ni	Cr	Mo	Cu	Sn	Fe
0.39	0.41	0.31	0.42	0.025	bal.

TABLE II

Parameters of EN plating.

Step	Process	Working condition
1	nickel strike	nickel salt: 240 g/L HCl: 80 g/L temperature: about 25 °C voltage: 7 V plating time: 1 min
2	EN plating	nickel salt: 80 g/L pH: 4.5–5.0 temperature: about 88 °C plating time: 70 min
3	heat treatment	temperature: 250 °C heating time: 2 h

3. Results and discussion

Figure 1 shows the observation of the cross section of EN plated gray cast iron. The EN coating was applied quite uniformly at a thickness of around 6 μm on the entire surface and the Ni strike layer is around 1.5 μm thick and the EN plated layer is around 4.5 μm thick. In general, EN coating is greatly affected by the microstructure of the substrate. In particular, in the case of gray cast iron, the microstructure acts as a barrier factor during EN plating because flake graphite is exposed on the surface. Nevertheless, no defect such as pores is found in the junction between the EN coating and the substrate by the Ni strike process. Therefore, the plated layer is expected to show excellent adhesion and corrosion resistance. The surface hardness of the EN plated layer was measured as 299 $HV_{1.0}$ and increased by around 37.5% to 411 $HV_{1.0}$ after heat treatment. The reason why the hardness increases after heat treatment is that in cases where the P content of the EN coating is 7 wt% or higher, an amorphous structured plated layer is formed through the coating [2], and when heat treatment is applied to the plated layer later, Ni_3P and Ni crystal phases are formed on the amorphous matrix so that the plated layer undergoes precipitation hardening leading to remarkable increases in the hardness [3–6]. The EN plated layer used in the present study consists of 8−10% P and 90−92% Ni and the heat treatment was implemented for two hours at 250 °C followed by slow furnace cooling. Increasing hardness of the EN plated layer through heat treatment has been identified to be effective in reducing cavitation damage so that positive results can be also expected in the present study [7–9].

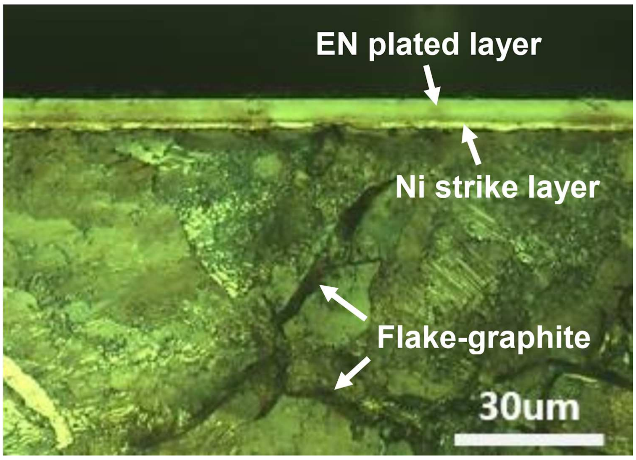

Fig. 1. Cross section of EN plated gray cast iron after etching by 4% nitric acid solution.

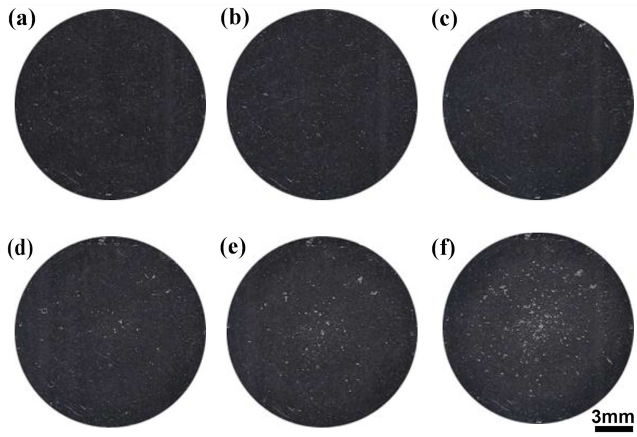

Fig. 2. Surface morphologies of EN plated specimen with cavitation erosion time: (a) as-received, (b) 30 min, (c) 60 min, (d) 120 min, (e) 180 min, (f) 240 min.

Figure 2 demonstrates the observation of the surface shapes of the EN plated specimens with cavitation erosion time in a coolant. Up to 60 min of the cavitation erosion time, no visually identifiable damage was observed on the surface. As surface damage, pits began to occur in the central part of the specimen when cavitation erosion time of 120 min had passed and the number of pits gradually increased with cavitation erosion time. These pits showed a pattern to gradually progress outward from the central part of the specimen with cavitation erosion time.

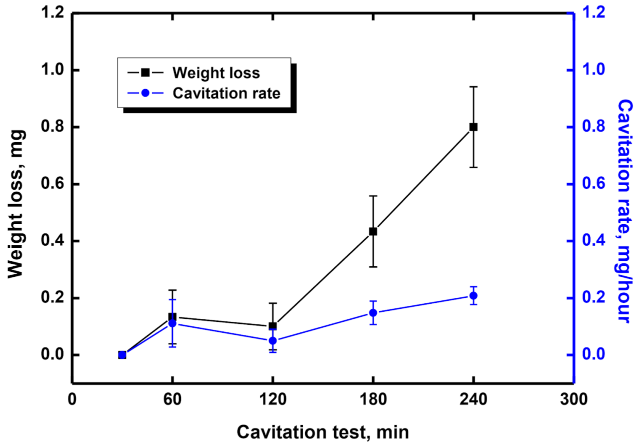

Fig. 3. Weight loss and cavitation rate of EN plated specimens with cavitation erosion time.

Therefore, the highest density of the pits occurred was observed in the central part of the specimen. According to the results of studies by Diodati et al. [10] and Won et al. [11], it can be seen that the reason why the cavitation damage is concentrated on the central part of the specimen is that the cavity cluster has a spray shape in the form of a trumpet-shaped column from the horn surface and shows a tendency to have the flow velocity and cavitation damage increasing toward the central part of the horn. In addition, the foregoing results are consistent with the results of a study conducted by Hanson and Morch indicating that the hemispheric cavity clusters formed on the horn surface intensively fail leading to the progress of surface damage [12].

Figure 3 is a graph that presents weight loss and cavitation rate of EN plated specimens with cavitation erosion time. Since almost no weight loss appears up to 120 min of cavitation erosion time, the 120 min section is judged to be the incubation period presented by Thiruvengadam [13]. In the case of cavitation damage, the shock waves and micro jets occurring when cavities collapse repeatedly hit the material surface leading to fatigue, failure, and material losses. In this case, the period before the fatigue effect due to the accumulation of cavitation shocks is called incubation period. Therefore, longer incubation periods means more excellent cavitation resistance. When cavitation erosion time of 120 min had passed, an acceleration period appeared in which the weight loss increased almost proportionally with cavitation erosion time. The cavitation damage rate was shown to be almost constant with cavitation erosion time and in the case of cavitation erosion time of 240 min with the highest damage rate, the cavitation damage rate was measured to be very low as 0.2 mg/hour indicating that the cavitation resistance of EN coating is excellent.

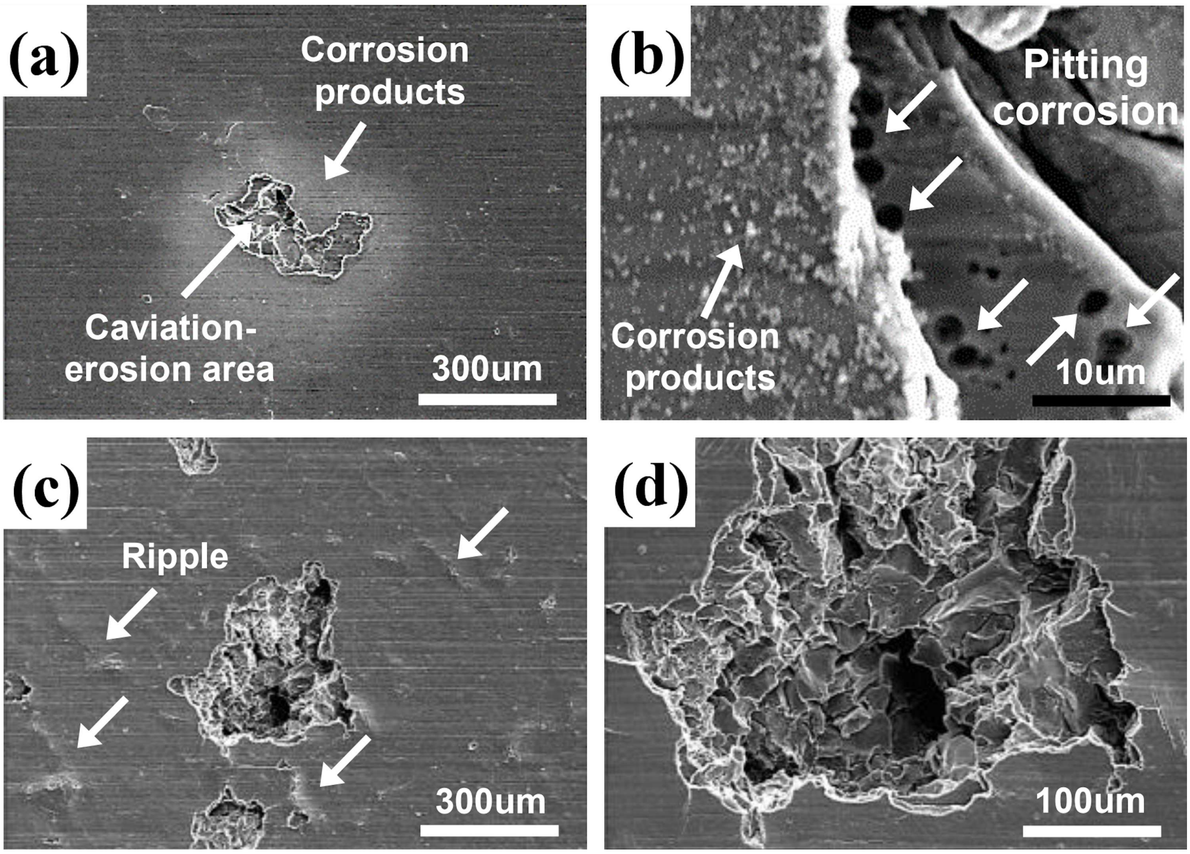

Fig. 4. Surface damage morphologies of EN plated specimen with cavitation erosion time; (a)–(b) 120 min and (c)–(d) 240 min.

Figure 4 presents a photo of the surface damage tendency of EN plated specimens with cavitation erosion time in a coolant observed by SEM. As shown in Fig. 4a, at cavitation erosion time of 120 minutes, the substrate was partially exposed due to locally occurred pit damage but only the EN plated layer was peeled off so that the damage progressed in the width direction. However, as shown in the area indicated by arrows in Fig. 4b, pitting corrosion appeared in the substrate adjacent to the boundary between the exposed substrate and the EN plated layer. This is considered attributable to the fact that the substrate exposed in a local and relatively small area due to cavitation damage and the EN plated layer in a relatively large area formed galvanic cells in the pattern of a small anode-a large cathode, and exposed to the cavitation environment to promote corrosion damage. In particular, metal surfaces exposed to a cavitation environment are known to show drastic increases in the corrosion rate due to the high temperature resulting from cavity collapse and the smooth oxygen supply following the formation of turbulence [9, 14]. Therefore, anodic dissolution reactions were promoted in the substrate exposed to the boundary area and the areas around pits in the EN plated layer were judged to have been observed as being bright because of the corrosion product formed by the hydrogen reduction reactions. At cavitation erosion time of 240 minutes, the damage to the substrate exposed to the inside of the pit became prominent with increases in their sizes and depths to form craters. In the case of low magnification photos, ripples were observed because the EN plated layer surfaces around the damage area were plastic deformed by the cavitation impact pressure (Fig. 4c). On the contrary, corrosion damage was not observed any longer in the damage area in high magnification photos (Fig. 4d). This is considered attributable to the fact that not only the physical damage to the substrate progressed much faster than the corrosion damage but also the effects of galvanic cells decreased as the exposed area of the substrate increased. Consequently, in the case of EN coating, local pitting damage is caused by cavitation attacks and galvanic corrosion accompanies the damage to accelerate the erosion damage. EN coating was plastic deformed due to continued cavitation attacks and showed a tendency to eventually fail due to accumulated fatigue. The exposed substrate by cavitation damage showed a pattern of cavitation damage progressing in the depth direction because cavitation attacks were concentrated.

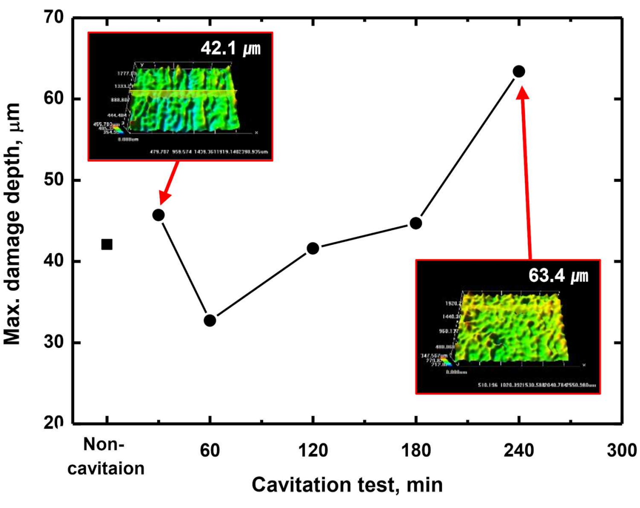

Fig. 5. 3D microscope analysis of surface damage of EN plated specimens with cavitation erosion time.

Figure 5 exhibits a graph of surface damage depths drawn after analyzing the surface damage of EN plated specimens in a coolant with cavitation erosion time using a 3D microscope. The surface damage depth showed a tendency to increase in general with cavitation erosion time. Unusually, however, at cavitation erosion time of 60 minutes, the surface damage depth was measured to be smaller than the substrate damage depth. This is judged attributable to the fact that as the uneven bumps formed on the EN coating surface during the plating process were removed so that the EN coating surface becomes evener than the substrate. Therefore, as shown in Fig. 3, the weight loss showed a tendency to temporarily increase a little at cavitation erosion time of 60 minutes. Thereafter, as the pits formed on the surface continuously grew with cavitation erosion time, the surface damage depth showed a tendency to increase. Eventually, when the experiment was completed, due to the tendency of local pitting damage, the maximum damage depth of 63.4 μm, which is larger by 21.3 μm than the damage depth on the substrate, was observed on the EN coating surface.

4. Conclusion

In this study, cavitation erosion experiments were conducted in a diesel engine coolant to understand the tendency of cavitation erosion damage to EN plated cylinder liners and the following results were obtained.

1. Through a Ni strike process, even EN coating could be formed without being affected by the microstructure of the substrate.
2. In the case of cavitation attacks, after the incubation period, EN coating developed into the acceleration period due to the occurrence and growth of pitting damage.
3. The initial pitting damage to EN coating was accompanied by galvanic corrosion so that it was accelerated.
4. Cavitation attacks were concentrated on the local pitting damage on EN coating so that the local pitting damage progressed in the depth direction and the surface damage depth increased.

Acknowledgments

This research was a part of the project titled “Construction of eco-friendly Al ship with painting, and maintenance/repairment free”, funded by the Ministry of Oceans and Fisheries, Korea.

References

[1] H.K. Junker, *Pistons and Engine Testing*, 1st ed., Springer Science & Business Media Verlag, Berlin 2012.

[2] T. Yamasaki, H. Izumi, H. Sunada, *Scr. Metall.* **15**, 177 (1981).

[3] S.H. Park, D.N. Lee, *J. Mater. Sci.* **23**, 1643 (1988).

[4] P.S. Kumar, P.K. Nair, *J. Mater. Process. Technol.* **56**, 511 (1996).

[5] I. Apachitei, J. Duszczyk, L. Katgerman, P.J.B. Overkamp, *Scr. Metall.* **38**, 1347 (1998).

[6] W. Reidel, *Electroless Nickel Plating*, 2nd ed., Cambridge Scientific Abstracts, Cambridge 1911.

[7] C.J. Lin, J.L. He, *Wear* **259**, 154 (2005).

[8] C.J. Lin, K.C. Chen, J.L. He, *Wear* **261**, 1390 (2006).

[9] W.J. Tomlinson, M. Girardi, *Surf. Coat. Tech.* **31**, 213 (1987).

[10] P. Diodati, G. Giannini, *Ultrason. Sonochem.* **8**, 49 (2001).

[11] D.S. Won, K.S. Jeon, Y.T. Kho, J.H. Lee, *Corros. Sci. Technol.* **23**, 215 (1994)

[12] I. Hansson, K.A. Mørch, *J. Appl. Phys.* **51**, 4651 (1980).

[13] A. Thiruvengadam, H.S. Preiser, *J. Ship Res.* **8**, 39 (1964)

[14] J. González-García, V. Sáez, I. Tudela, M.I. Díez-Garcia, M. Deseada Esclapez, O. Louisnard, *Water* **2**, 28 (2010).